back control, considerations of sensor location as well as technology and other features of the physical problem are typically more important than compensator transfer-function design.

7.3 LATERAL AND LONGITUDINAL CONTROL OF A BOEING 747

The Boeing 747 is a large, wide-body jet transport airplane. A picture of a Boeing 747 is shown in Fig. 7.28, and a schematic with the relevant coordinates is shown in Fig. 7.29. The linearized equations of (rigid-body) motion for the Boeing 747 are of eighth-order but are separated into two fourth-order sets representing the longitudinal (u, w, q in Fig. 7.29) and lateral motion (β, r, p in Fig. 7.29). The longitudinal motion consists of axial, vertical, and pitching motion (see Section 6.2), while the lateral motion consists of rolling, yawing, and lateral movement. The elevator control surfaces and the throttle affect the longitudinal motion, whereas the aileron and rudder primarily affect lateral-directional motion. Although there is a small amount of coupling of lateral motion into longitudinal motion, this is usually ignored and the equations of motion are treated as two decoupled fourth-order sets for designing the control, or *stability augmentation*, for the aircraft. We will discuss the design of a stability-augmentation system for the lateral dynamics, called a *yaw damper*, and certain aspects of the autopilot having influence over the longitudinal behavior.

7.3.1 Yaw Damper

STEP 1: *Understand the process and its performance specifications.* Swept-wing aircraft have a natural tendency to be lightly damped in one of the lateral modes of motion. At typical commercial-aircraft cruising speeds

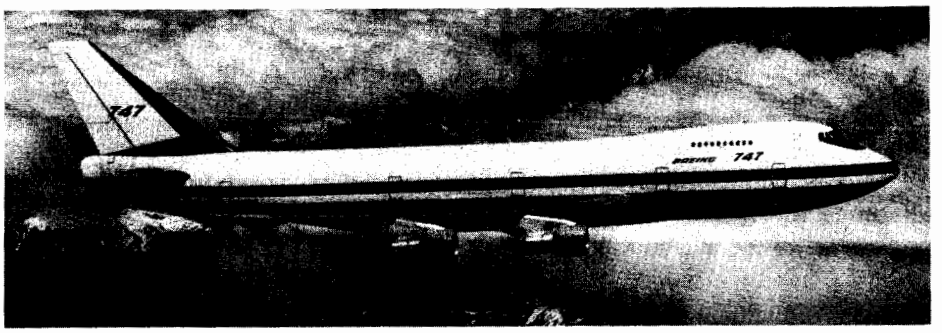

FIGURE 7.28
Boeing 747 aircraft. (*Courtesy Boeing Commercial Airplane Co.*)

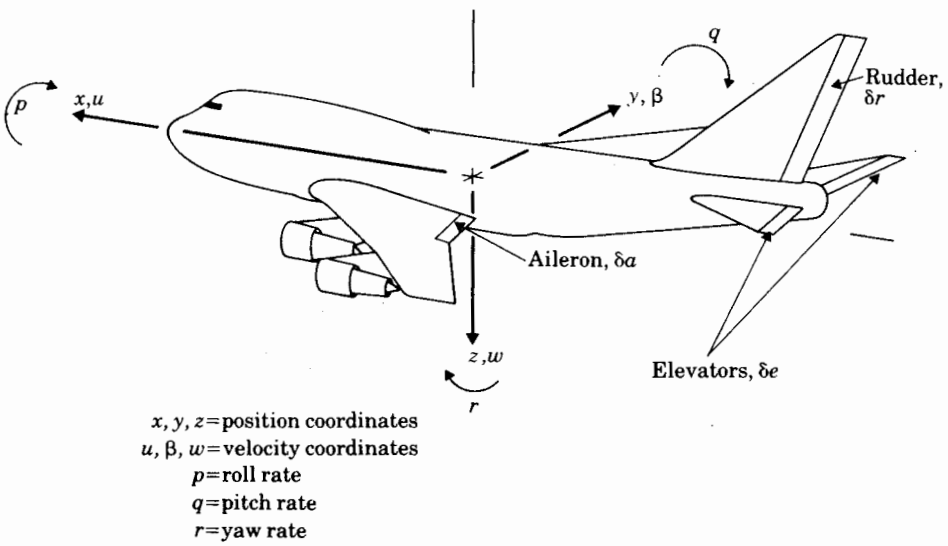

FIGURE 7.29
Definition of aircraft coordinates.

and altitudes, this mode is sufficiently difficult for pilots to control that virtually every swept-wing aircraft has a feedback system to help the pilot. The specification of our control system is, therefore, to modify the natural dynamics so that the plane is pleasant for the pilot to fly. Studies have shown that pilots like natural frequencies $\lesssim 1$ rad/s with a damping ratio of $\zeta \gtrsim 0.5$. Aircraft with dynamics that violate these guidelines are generally considered fatiguing to fly and highly undesirable. Our system specifications, therefore, are to achieve lateral dynamics that meet these root constraints.

STEP 2: *Select a sensor.* The easiest measurement to take of aircraft motion is that of angular rate. Velocities can also be measured using pitot tubes and wind-vane devices, but these are noisier and less reliable for stabilization. Two angular rates—roll and yaw—partake in the lateral motion. Study of the lightly damped lateral mode indicates that it is primarily a yawing phenomenon; thus measurement of the yaw rate is a logical starting point for the design. Up until the early 1980s, the measurement had been made with a gyroscope, essentially a small, fast-spinning rotor that can yield an electric output proportional to the angular yaw rate of the aircraft. Since the early 1980s, most new aircraft systems are relying on a laser device (called a *ring-laser gyroscope*) for the measurement. Here, two laser beams traverse a closed path (often a triangle) in opposite directions. As the triangular device rotates, the apparent frequency of the two beams shifts, and this frequency

shift is measured, producing a measure of the rotational rate. These devices have fewer moving parts and are more reliable at less cost than the spinning-rotor variety of gyroscope.

STEP 3: *Select an actuator.* Two aerodynamic surfaces typically influence the lateral aircraft motion: the rudder and the ailerons (see Fig. 7.29). The lightly damped yaw mode that is being stabilized by the yaw damper is most affected by the rudder. Therefore, use of that single control input is a logical starting point for the design. Hydraulic devices are universally employed in large aircraft to provide the force that moves the aerodynamic surfaces. No other kind of device has been developed to provide the combination of high force, high speed, and light weight that is desired for the actuation of the controlling aerodynamic surfaces. On the other hand, the low-speed flaps, which are extended slowly prior to landing, are typically actuated by an electric motor with a worm gear.

For small aircraft with no stabilization system, no "actuator" is required at all; the pilot wheel is directly connected to the aerodynamic surface via wire cables, and all the force required to move the surface is provided by the pilot.

STEP 4: *Make a linear model.* The lateral perturbation equations of motion in horizontal flight at 40,000 ft and forward speed $U = 774$ ft/s (mach 0.8) are[†] (Heffley and Jewell, 1972)

$$\begin{bmatrix} \dot{\beta} \\ \dot{r} \\ \dot{p} \\ \dot{\phi} \end{bmatrix} = \begin{bmatrix} -0.0558 & -0.9968 & 0.0802 & 0.0415 \\ 0.598 & -0.115 & -0.0318 & 0 \\ -3.05 & 0.388 & -0.4650 & 0 \\ 0 & 0.0805 & 1 & 0 \end{bmatrix} \begin{bmatrix} \beta \\ r \\ p \\ \phi \end{bmatrix} + \begin{bmatrix} 0.0729 \\ -4.75 \\ 1.53 \\ 0 \end{bmatrix} \delta r$$

$$y = \begin{bmatrix} 0 & 1 & 0 & 0 \end{bmatrix} \begin{bmatrix} \beta \\ r \\ p \\ \phi \end{bmatrix}. \tag{7.17}$$

The transfer function is

$$G(s) = \frac{r(s)}{\delta r(s)} = \frac{-0.475(s + 0.498)(s + 0.012 \pm j0.488)}{(s + 0.0073)(s + 0.563)(s + 0.033 \pm j0.947)} \tag{7.18}$$

so that the system has two stable real poles and a pair of stable complex poles referred to as the "Dutch roll," the name coming from the motions of a person skating on the frozen canals of Holland. The stable real poles are referred to as the *spiral mode* ($s_1 = -0.0073$) and the *roll mode* ($s_2 = -0.563$): From looking at the natural roots, we see that the offending mode that needs repair

[†]The units for β and ϕ are radians, and for r and p the units are radians per second.

for good pilot handling is the Dutch roll, or the roots at $s = -0.033 \pm j0.95$. The roots have an acceptable frequency, but their damping of $\zeta \cong 0.03$ is far short of the desired $\zeta \cong 0.5$.

STEP 5: *Try a lead-lag or PID design.* As a first crack at the design, proportional feedback of the yaw rate to the rudder will be considered. The root locus versus the gain of this feedback is shown in Fig. 7.30, and its frequency response is shown in Fig. 7.31. The figures show that a damping of $\zeta \cong 0.45$ is achievable.

In practice, however, it is found that this simple feedback creates an objectionable quality during a steady turn, since it provides a steady rudder input opposite the pilot's input due to the steady yaw rate. This dilemma is solved by the addition of a *washout circuit* in the feedback. The washout

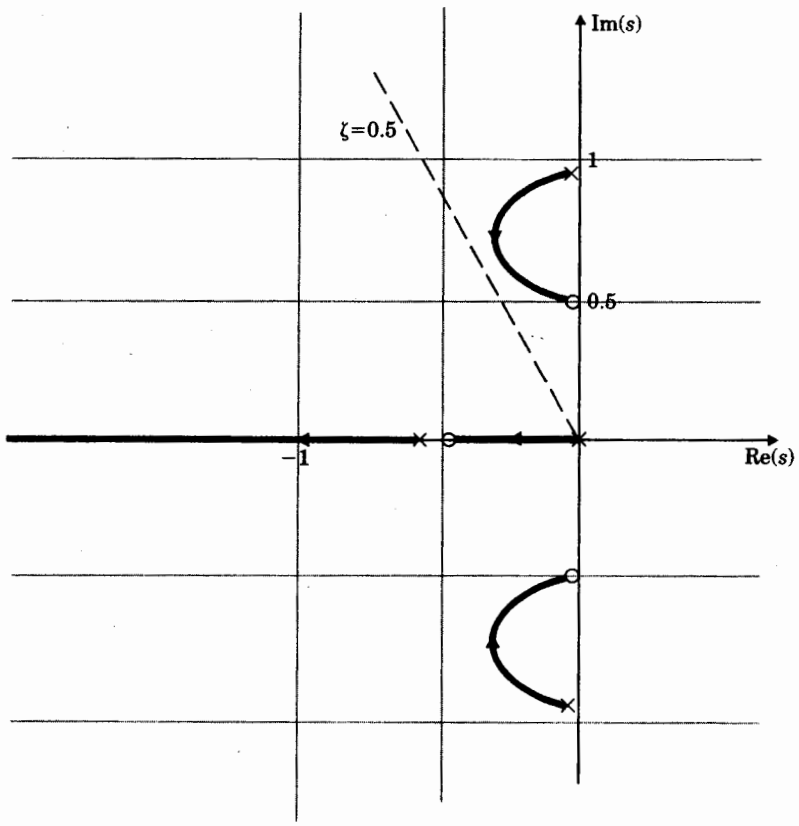

FIGURE 7.30
Root locus for yaw damper with direct feedback.

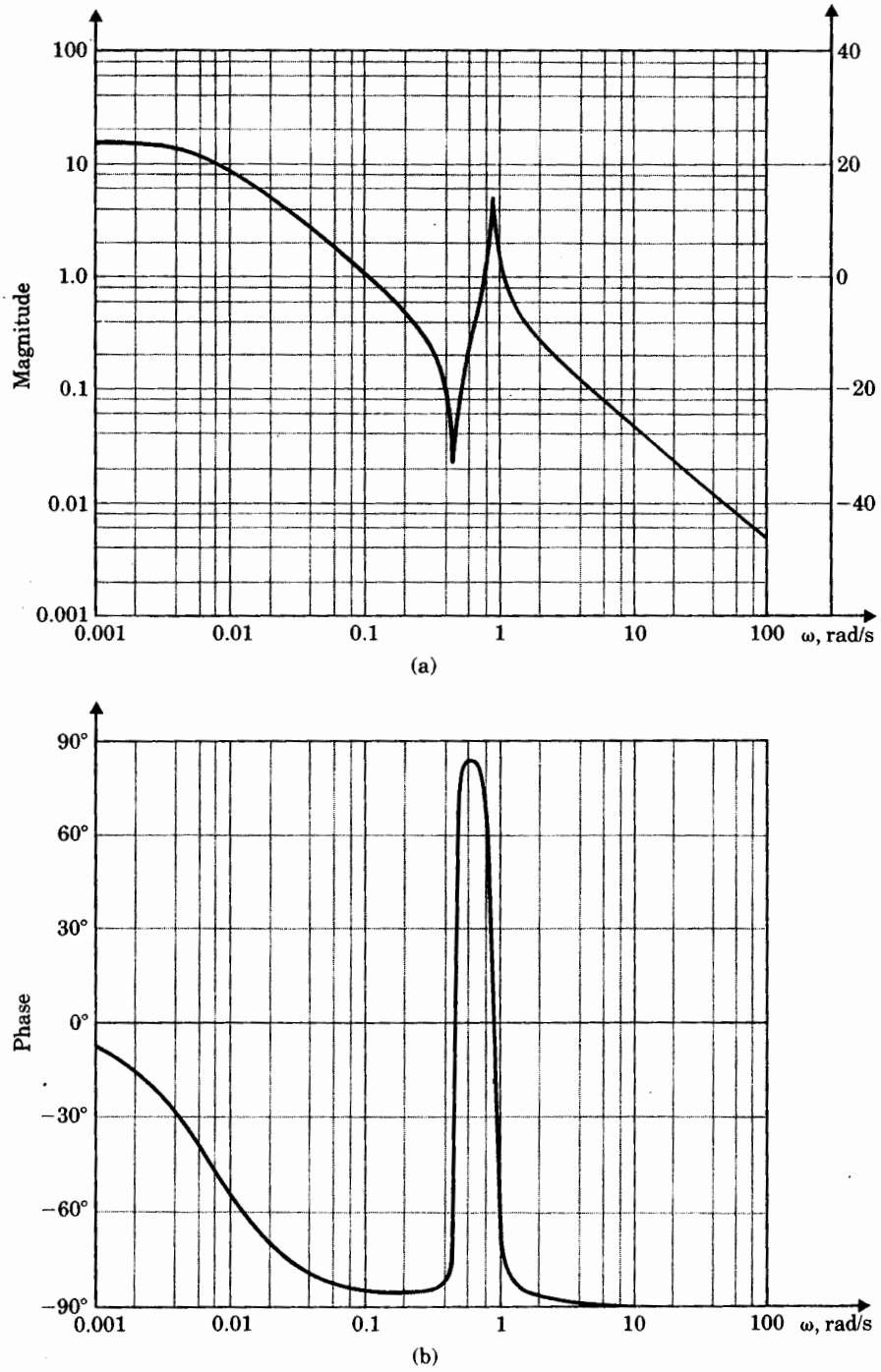

FIGURE 7.31
Frequency response of yaw damper with direct feedback: (a) magnitude and (b) phase.

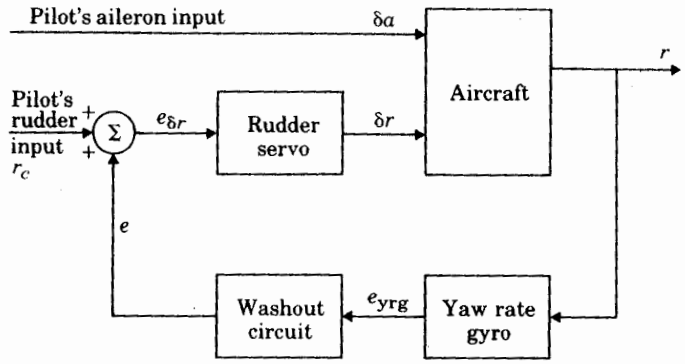

(a)

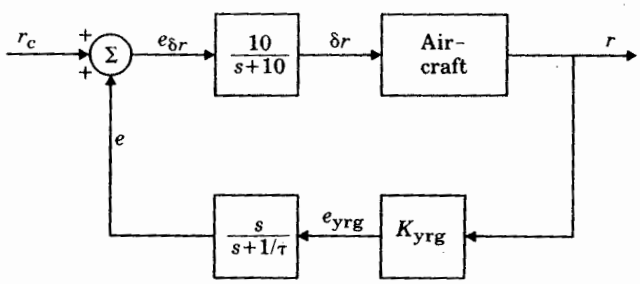

(b)

FIGURE 7.32
Yaw damper: (a) block diagram and (b) block diagram for analysis.

circuit has the feature that it passes only transient inputs and "washes out" steady and low-frequency inputs. Figure 7.32 shows a block diagram of the yaw damper with the washout included.

The transfer function of the washout circuit is

$$H(s) = \frac{e(s)}{e_{yrg}(s)} = \frac{s}{s + (1/\tau)}.$$

FIGURE 7.33
Frequency response of the washout circuit: (a) magnitude, (b) phase, and (c) step response.

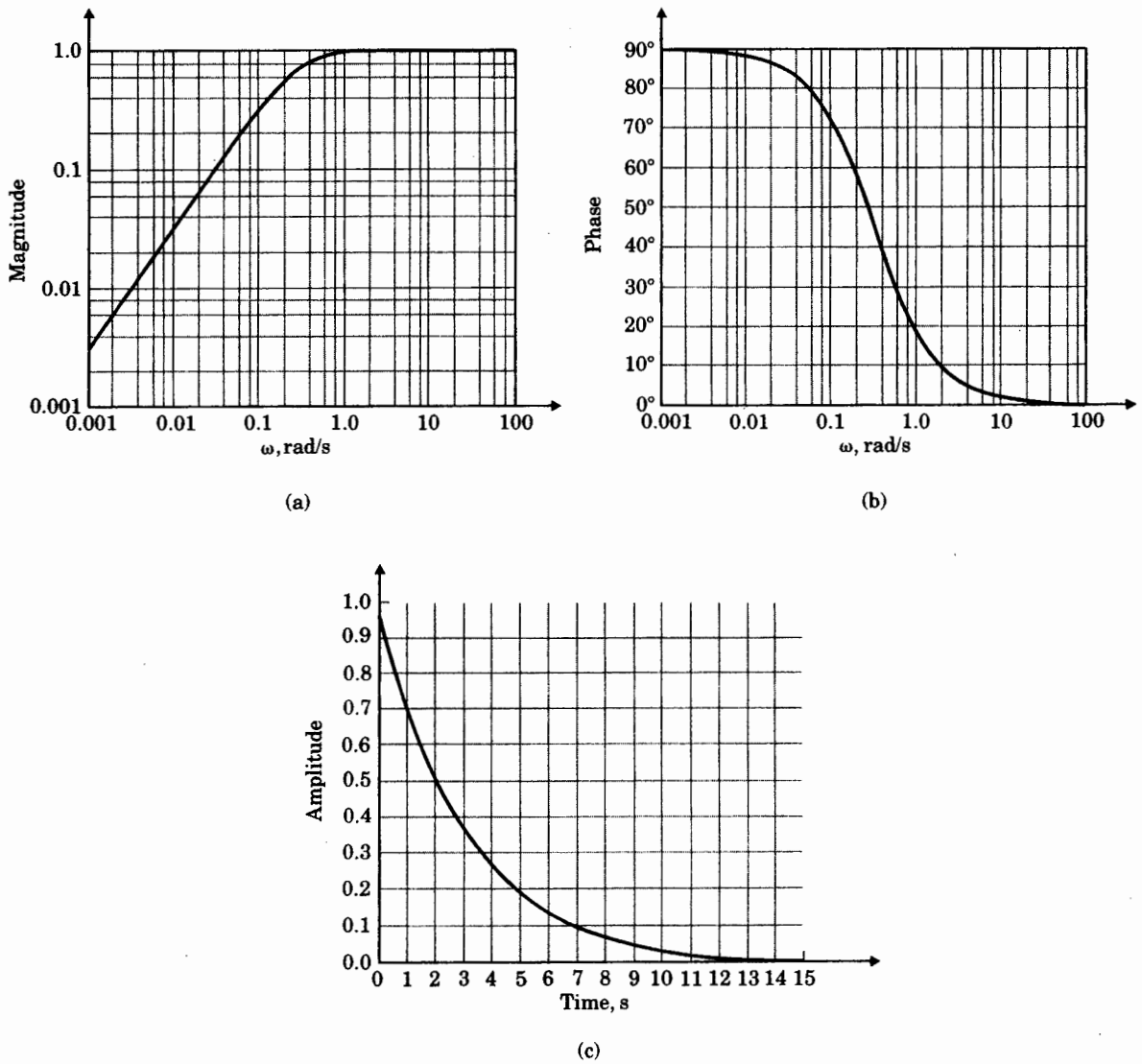

The frequency response of the washout circuit is shown in Fig. 7.33(a and b) for $\tau = 3$ s, and its response to a unit step input is shown in Fig. 7.33(c). The root locus of the system with washout circuit is shown in Fig. 7.34. As seen from the root locus, with the addition of the washout very little increase in the damping ratio can be obtained. The rudder servo represents the actuator dynamics

$$\frac{\delta r(s)}{e_{\delta r}(s)} = \frac{10}{s + 10},$$

which is fast compared with the dynamics of the system. The root locus of the system with washout and actuator dynamics is shown in Fig. 7.35. The associated frequency responses of the system are shown in Fig. 7.36. The response of the closed-loop system is an initial condition of $\beta_0 = 1°$ is shown in Fig. 7.37 for a root locus gain of unity. The root locus indicates that the maximum achievable damping with this feedback scheme is approximately $\zeta = 0.3$. [redacted] this is a considerable improvement over the original aircraft,

[redacted]

STEP 6: *Try an optimal design using pole placement.* If we augment the dynamic model of the system by adding the actuator and washout, we obtain the state-variable model:

$$\begin{bmatrix} \dot{x}_A \\ \dot{\beta} \\ \dot{r} \\ \dot{p} \\ \dot{\phi} \\ \dot{x}_{\omega_0} \end{bmatrix} = \left[\begin{array}{c|cccc|c} -10 & 0 & 0 & 0 & 0 & 0 \\ \hline 0.0729 & -0.0558 & -0.997 & 0.0802 & 0.0415 & 0 \\ -4.75 & 0.598 & -0.1150 & -0.0318 & 0 & 0 \\ 1.53 & -3.05 & 0.388 & -0.465 & 0 & 0 \\ 0 & 0 & 0.0805 & 1 & 0 & 0 \\ \hline 0 & 0 & 1 & 0 & 0 & -0.333 \end{array}\right]$$

$$\times \begin{bmatrix} x_A \\ \beta \\ r \\ p \\ \phi \\ x_{\omega_0} \end{bmatrix} + \begin{bmatrix} 10 \\ 0 \\ 0 \\ 0 \\ 0 \\ 0 \end{bmatrix} e_{\delta r},$$

$$e = \left[0 \mid 0 \;\; 1 \;\; 0 \;\; 0 \mid -0.333\right] \begin{bmatrix} x_A \\ \beta \\ r \\ p \\ \phi \\ x_{\omega_0} \end{bmatrix},$$

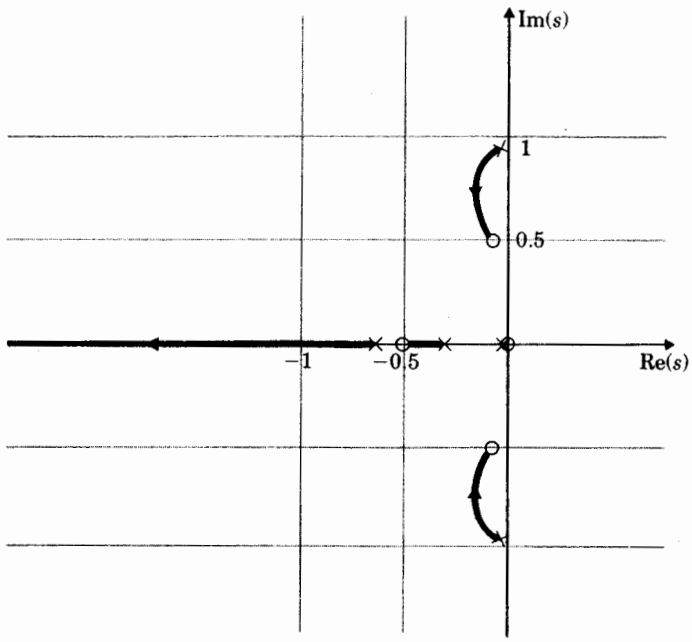

FIGURE 7.34
Root locus with washout circuit, $\tau = 3$.

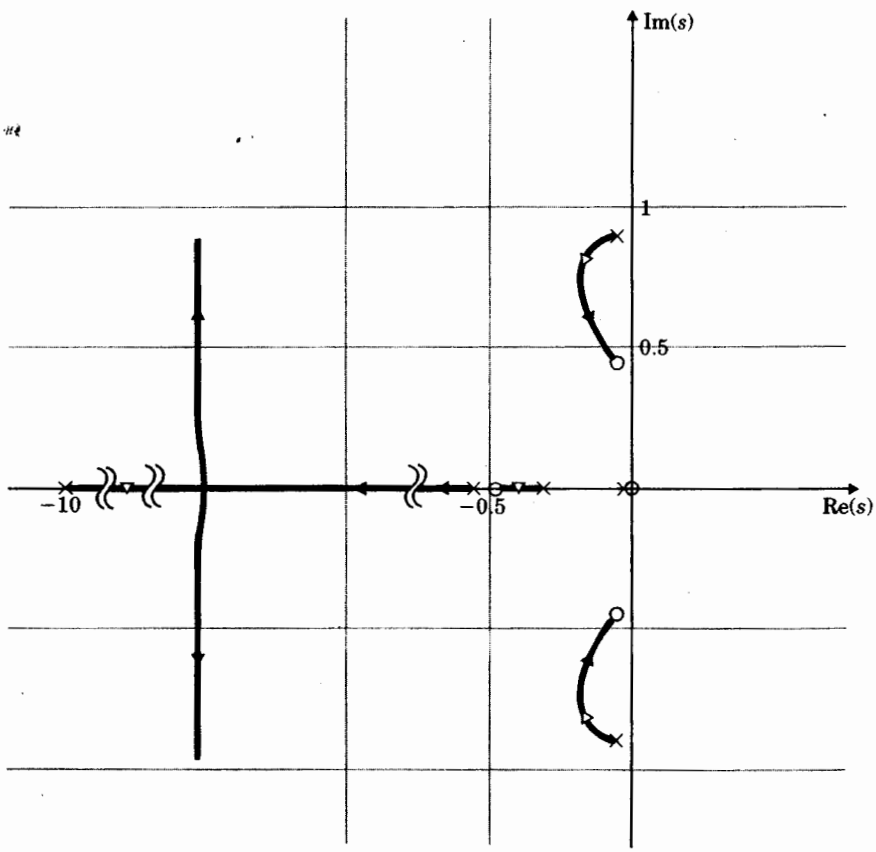

FIGURE 7.35
Root locus with washout circuit, $\tau = 3$, and actuator.

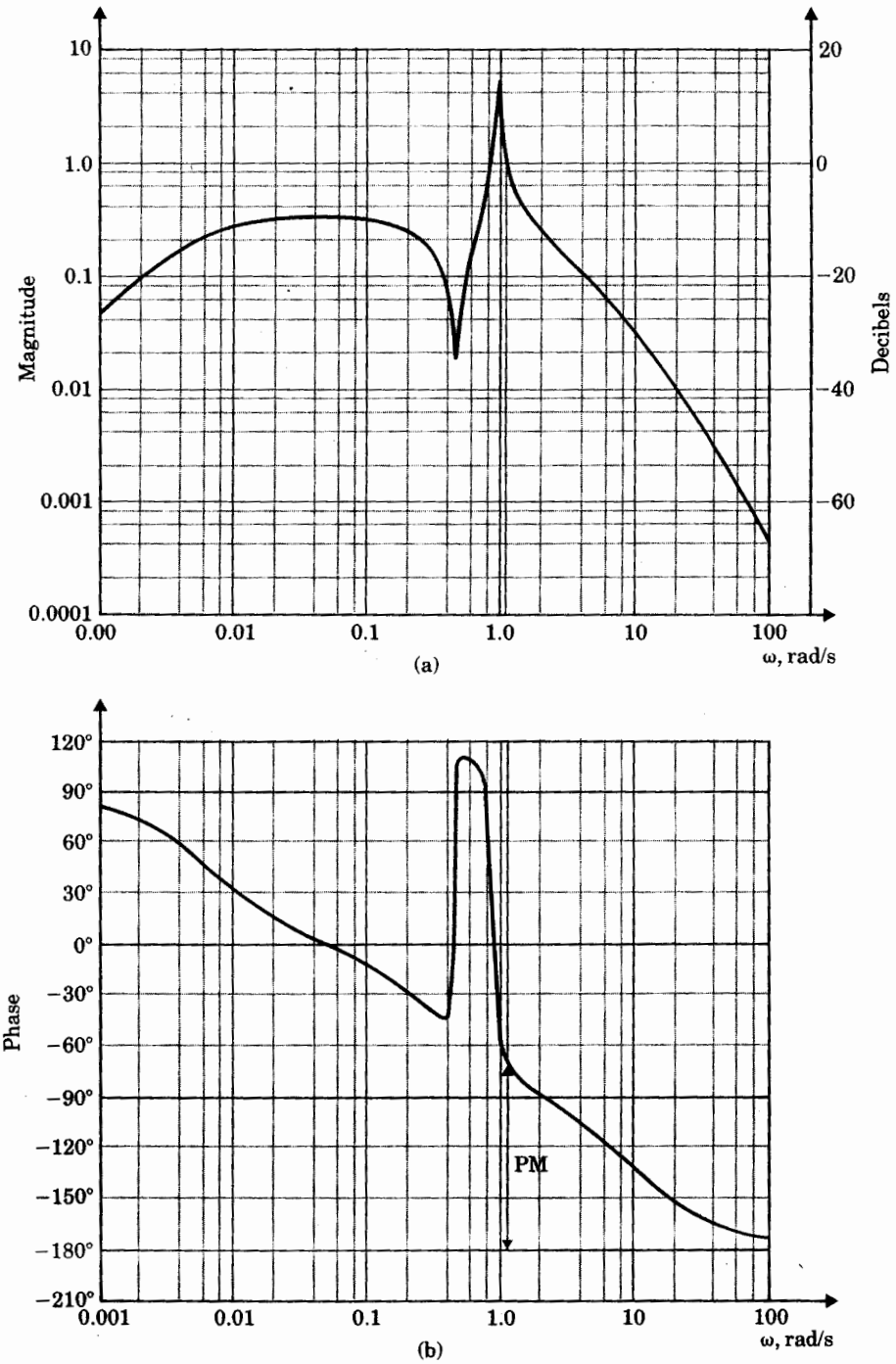

FIGURE 7.36
Frequency response of yaw damper, including washout and actuator: (a) magnitude and (b) phase.

Re(s)

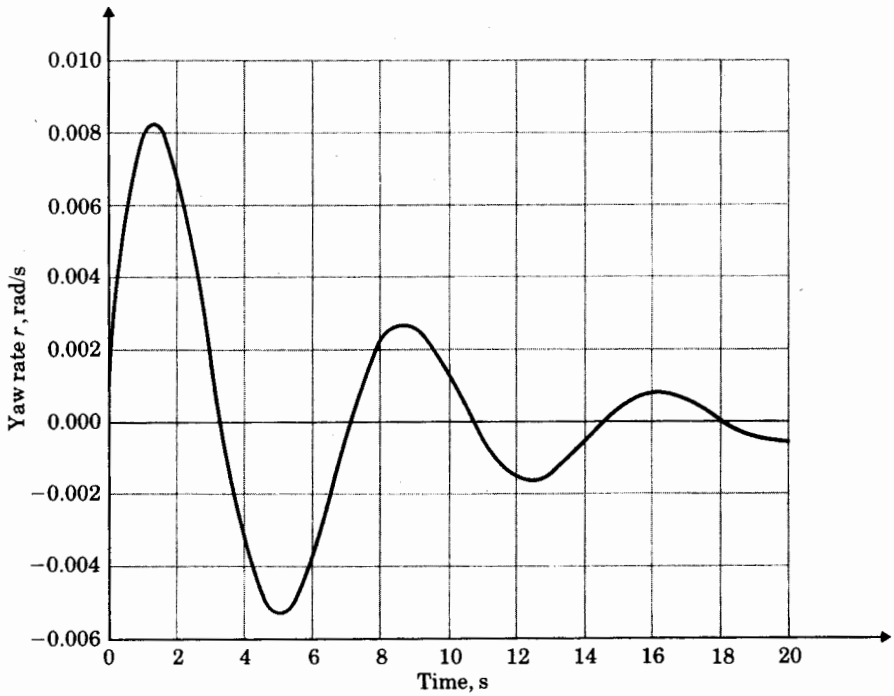

FIGURE 7.37
Initial condition response for $\beta_0 = 1°$.

where e_{δ_r} is the input to the actuator and e is the output of the washout. The symmetric root locus for the augmented system is as shown in Fig. 7.38. If we select the state feedback poles from the symmetric root locus so that the complex roots have maximum damping ($\zeta = 0.4$), we find

$$\alpha_c(s) = (s + 0.0051)(s + 0.468)(s + 0.279 \pm \zeta 0.628) \times (s + 1.106)(s + 9.89),$$

then the state feedback gain is computed to be

$$\mathbf{K} = [1.059 \quad | \quad -0.191 \quad -2.32 \quad 0.00992 \quad 0.0370 \quad | \quad 0.486].$$

Note that the third entry in $\mathbf{K}$ is larger than the others so that the feedback of all four states is essentially the same as proportional feedback of r. This is also evident from the similarity of the root locus in Fig. 7.30 and the SRL of Fig. 7.38. If we select the estimator poles to be five times faster than the controller poles, that is,

$$\alpha_e(s) = (s + 0.0253)(s + 2.34)(s + 1.39 \pm j3.14) \times (s + 5.53)(s + 49.5),$$

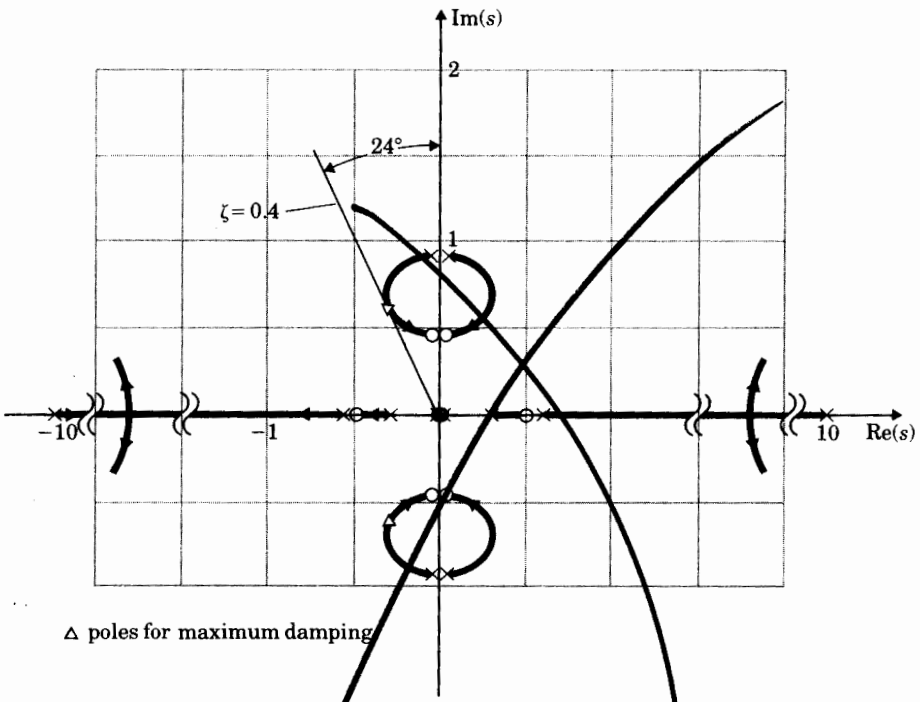

GURE 7.38
ymmetric root locus
f lateral dynamics,
cluding washout filter
nd actuator.

then the estimator gain is found to be

$$\mathbf{L} = \begin{bmatrix} 25.0 \\ -2044 \\ -5158 \\ -24843 \\ -40113 \\ -15624 \end{bmatrix}.$$

The compensator transfer function from Eq. (6.113) is

$$G_c(s) = \frac{-844(s + 10.0)(s - 1.04)(s + 0.974 \pm j0.859)(s + 0.0230)}{(s + 0.0272)(s + 0.837 \pm j0.671)(s + 4.07 \pm j10.1)(s + 51.3)}. \quad (7.19)$$

Figure 7.39 shows the response of the system to an initial condition of $\beta_0 = 1°$. It is clear from the root locus that the damping can be improved by the SRL approach, and this is borne out by the reduced oscillatory behavior in the transient response of the system. However, this improvement has come at a

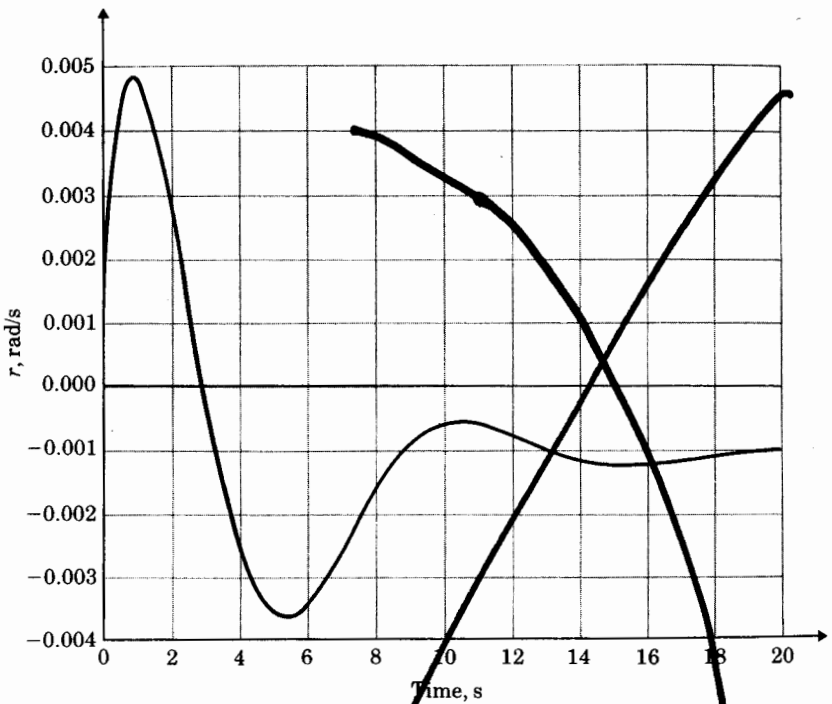

FIGURE 7.39
Initial condition response for $\beta_0 = 1°$, $\hat{x}_0 = 0$.

considerable price. Note that the order of the compensator has increased from 1 in the original design (Fig. 7.32) to 6 in the design obtained using the controller/estimator/SRL approach.

Aircraft yaw dampers in use today generally employ a proportional feedback of yaw rate to rudder through a washout or through minor modifications to this design. The improved performance achievable with an optimal design approach utilizing full-state feedback and estimation is not judged worth the increase in complexity.

Perhaps a more fruitful approach to improvement of the design would be to add the aileron surface as a control variable along with the rudder. However, this approach, too, has not been considered worth its complexity.

STEPS 7 AND 8: *Verify the Design.* Linear models of aircraft motion are reasonably accurate as long as the motion is small enough that the actuators and surfaces do not saturate. But since actuators are sized for safety so that they handle large transients, their saturation is very rare. The linear-analysis-

based design is, therefore, reasonably accurate, and we will not pursue a nonlinear simulation or further design verification.

7.3.2 Altitude-Hold Autopilot

STEP 1: *Understand the process and its performance specifications.* One of the pilot's many tasks is to hold a specific altitude. As an aid to keeping aircraft from colliding, those craft on an easterly path are required to be on an odd multiple of 1000 ft, while those on a westerly path are required to be on an even multiple of 1000 ft. It is therefore of some concern to the pilot that the altitude be held to within a few hundred feet. A well-trained attentive pilot can easily accomplish this task to within ± 50 ft, and this kind of tolerance is what the air-traffic controllers expect pilots to maintain. Since this task requires the pilot to be fairly diligent, sophisticated aircraft often have an "altitude-hold autopilot" to perform the task. This system is fundamentally different from the yaw damper in that its role is to replace the pilot for certain periods of time, while the yaw damper's role is to help the pilot fly. Dynamic specifications, therefore, need not be such that pilots like the craft's "feel"; instead, the design should provide the kind of ride that pilots and passengers like. The damping ratio should still be in the vicinity of $\zeta \cong 0.5$, but, for a smooth ride, the natural frequency should be much slower than 1 rad/s.

STEP 2: *Select a sensor.* Clearly needed is a device to measure altitude, a task most easily done by measuring the atmospheric pressure. Almost from the time of the first Wright brothers' flight, this basic idea has been used in a device called a *barometric altimeter*. Before autopilots, the device consisted of a bellows whose free end was connected to a needle that directly indicated altitude on a dial. The same idea is used today, but the pressure is sensed electrically.

Because altitude control is essentially four integrations from the controlling elevator input, stabilization of the feedback loop cannot be accomplished by simple proportional feedback. Therefore pitch rate q is also used as a stabilizing feedback; it is measured by a gyroscope or ring-laser gyro identical to that used for yaw-rate measurement. Further stabilization from pitch-angle feedback is also helpful. It is obtained from either a ring-laser gyro inertial reference system or a "rate-integrating gyro," a device similar to the rate gyro, but structured differently so that its outputs are proportional to the angle of the aircraft's pitch (θ) and roll angles (ϕ).

STEP 3: *Select an actuator.* The only aerodynamic surface typically used for pitch control on most aircraft is the elevator, δe. It is located on the horizontal tail, well removed from the aircraft's center of gravity so that its force produces an angular pitch rate and thus angle, which act to change the

lift from the wing. In some high-performance aircraft, there are "direct-lift" control devices on the wing or perhaps small "canard" surfaces forward of the wing, which produce vertical forces on the aircraft much faster than elevators are able to. However, for purposes of our altitude hold, we will only consider the typical case of an elevator surface on the tail.

As for the rudder, hydraulic actuators are the preferred device to move the elevator surface.

STEP 4: *Make a linear model.* The longitudinal perturbation equations of motion for the Boeing 747 in horizontal flight, $U = 830$ ft/s at 20,000 ft (mach 0.8) with a weight of 637,000 lb, are

$$\begin{bmatrix} \dot{u} \\ \dot{w} \\ \dot{q} \\ \dot{\theta} \\ \dot{h} \end{bmatrix} = \begin{bmatrix} -0.00643 & 0.0263 & 0 & -32.2 & 0 \\ -0.0941 & -0.624 & 820 & 0 & 0 \\ -0.000222 & -0.00153 & -0.668 & 0 & 0 \\ 0 & 0 & 1 & 0 & 0 \\ 0 & -1 & 0 & 830 & 0 \end{bmatrix} \begin{bmatrix} u \\ w \\ q \\ \theta \\ h \end{bmatrix} + \begin{bmatrix} 0 \\ -32.7 \\ -2.08 \\ 0 \\ 0 \end{bmatrix} \delta e, \tag{7.20}$$

where the desired output for an altitude-hold autopilot is

$$h = \begin{bmatrix} 0 & 0 & 0 & 0 & 1 \end{bmatrix} \begin{bmatrix} u \\ w \\ q \\ \theta \\ h \end{bmatrix}. \tag{7.21}$$

The system has two pairs of stable complex poles and a root at $s = 0$. The complex pair at $-0.003 \pm j0.0098$ are referred to as the *phugoid mode*[†] and the poles at $-0.6463 \pm j1.1211$ are the *short-period modes*.

STEP 5: *Try a lead-lag or PID controller.* As a first step in the design, it is typically helpful to use an inner-loop feedback of q to δe so as to improve the damping of the short-period mode of the aircraft (see Fig. 7.40). The transfer function from δe to q is

$$\frac{q(s)}{\delta e(s)} = \frac{-2.08s(s + 0.0105)(s + 0.596)}{(s + 0.003 \pm j0.0098)(s + 0.646 \pm j1.121)}. \tag{7.22}$$

The root locus for q feedback using Eq. (7.22) is as shown in Fig. 7.41. Since k_q is the root-locus parameter, the system matrix (Eq. 7.20) is now modified as follows:

$$\mathbf{F}_q = \mathbf{F} + k_q \mathbf{G}\mathbf{H}_q, \tag{7.23}$$

[†]The name was adopted by F. W. Lanchester (1908), who was the first to study the dynamic stability of aircraft analytically. It is apparently an incorrect version of a Greek word.

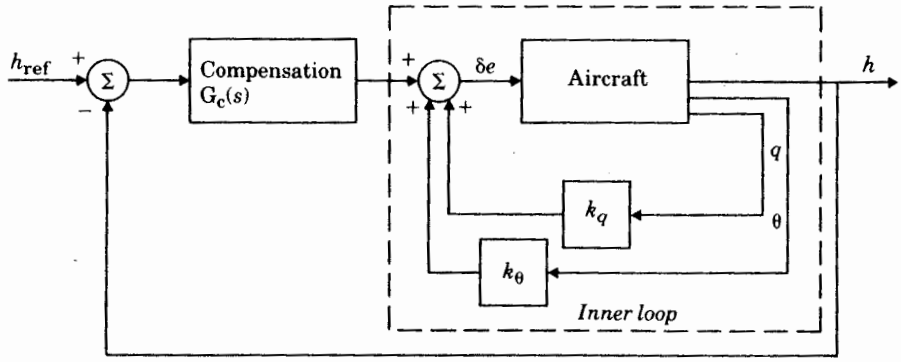

FIGURE 7.40
Altitude-hold feedback system.

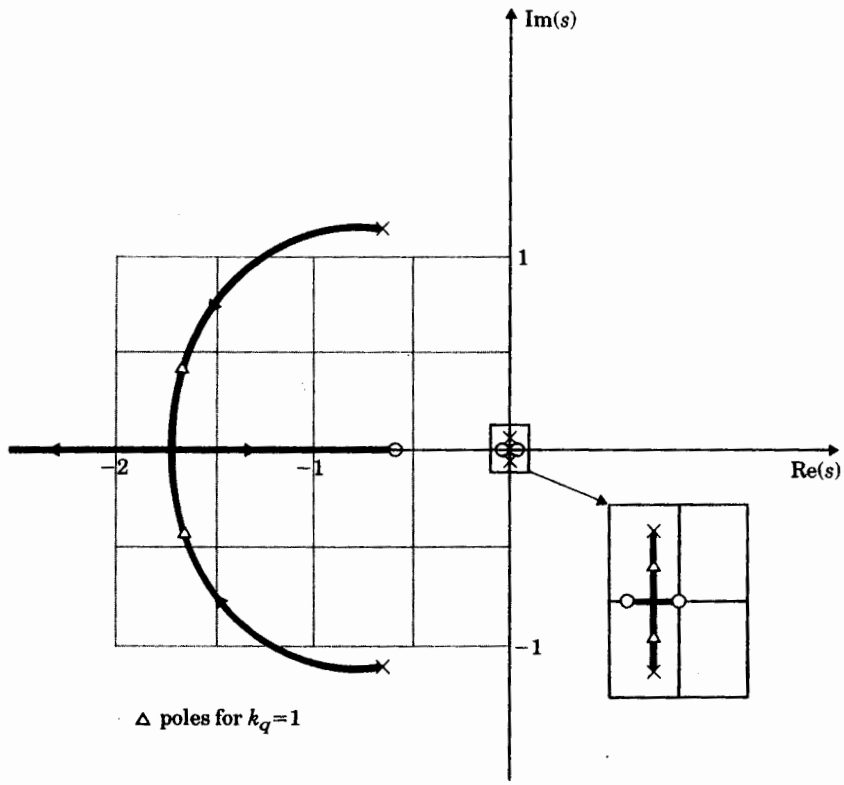

FIGURE 7.41
Root locus for longitudinal dynamics with q feedback.

where $\mathbf{F}$ and $\mathbf{G}$ are as defined in Eq. (7.20) and $\mathbf{H}_q = [0 \quad 0 \quad 1 \quad 0 \quad 0]$. The process of picking a suitable gain k_q is an iterative one. The selection procedure is the same one discussed in Chapter 4 (recall the continuation locus and tachometer feedback example in Section 4.6). If we choose $k_q = 1$, then the closed-loop poles are located at $-0.0039 \pm j0.0067$, $-1.683 \pm j0.277$ on the root locus and

$$\mathbf{F}_q = \begin{bmatrix} -0.00643 & 0.0263 & 0 & -32.2 & 0 \\ -0.0941 & -0.624 & 787 & 0 & 0 \\ -0.000222 & -0.00153 & -2.75 & 0 & 0 \\ 0 & 0 & 1 & 0 & 0 \\ 0 & -1 & 0 & 830 & 0 \end{bmatrix}.$$

Note that only the third column of $\mathbf{F}_q$ is different from $\mathbf{F}$. To further improve the damping, the pitch angle of the aircraft must be controlled. This is achieved by feeding back also the pitch angle (θ) to elevator control. If we

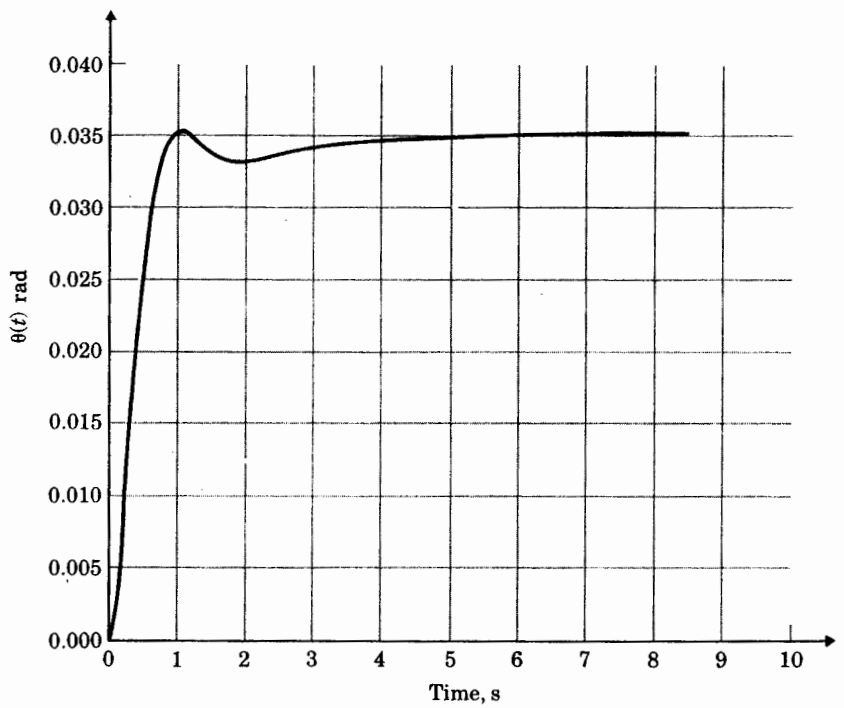

FIGURE 7.42
Response of an attitude-hold autopilot to a command in θ.

FIGURE 7.43
0° root locu
feedback o

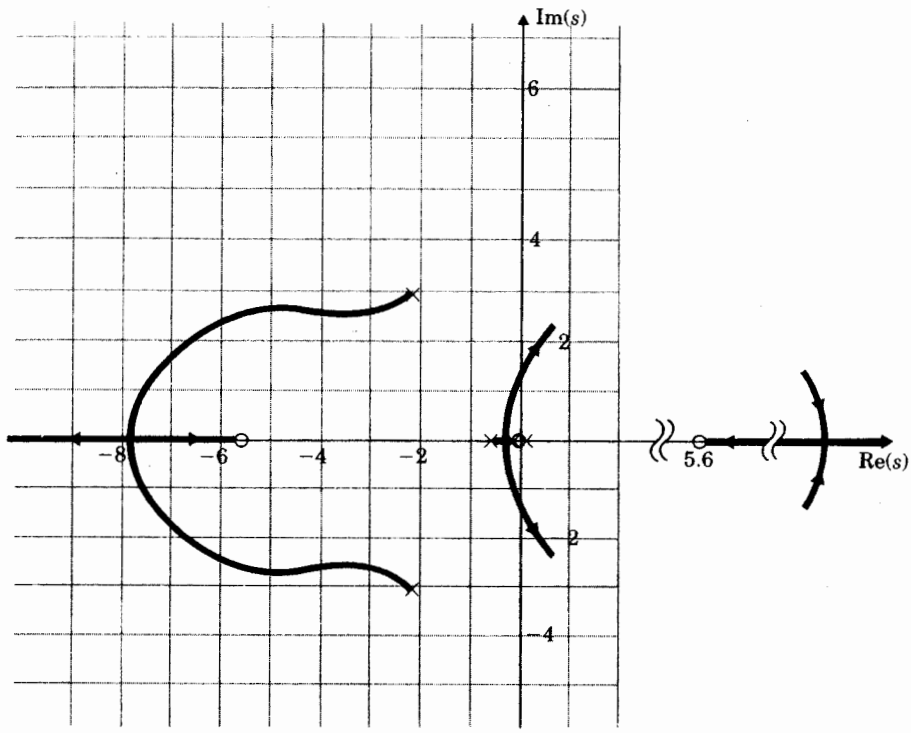

FIGURE 7.43
0° root locus with h feedback only.

select[†]

$$\mathbf{K}_{\theta q} = [0 \quad 0 \quad -0.8 \quad -6]$$

in order to feedback θ and q, then the system matrix is

$$\mathbf{F}_{\theta q} = \mathbf{F}_q - \mathbf{G}\mathbf{K}_{\theta q}$$

$$= \begin{bmatrix} -0.0064 & 0.0263 & 0 & -32.2 & 0 \\ -0.0941 & -0.624 & 761 & -196.2 & 0 \\ -0.0002 & -0.0015 & -4.41 & -12.48 & 0 \\ 0 & 0 & 1 & 0 & 0 \\ 0 & -1 & 0 & 830 & 0 \end{bmatrix}, \tag{7.24}$$

[†]A design based on SRL would suggest feeding back θ and q at this point.

with poles at $s = 0, -2.25 \pm j2.99, -0.531, -0.0105$. So far, the inner loop of the aircraft has been stabilized significantly. The uncontrolled aircraft has a natural tendency to return to level attitude as evidence by the phugoid roots at $s = -0.003 \pm j0.0098$. This inner stabilization is necessary to enable an outer h and $\dot{h}$ feedback to be successful; furthermore, the θ and q feedbacks can be used by themselves in an attitude-hold mode of an autopilot, where a pilot wishes to control θ directly through input command. Figure 7.42 shows the response of an attitude-hold autopilot to a 2° (0.035 rad) step command in θ. The transfer function of the system is now

$$\frac{h(s)}{\delta e(s)} = \frac{32.7(s + 0.0045)(s + 5.64)(s - 5.61)}{s(s + 2.25 \pm j2.99)(s + 0.0105)(s + 0.0531)}. \qquad (7.25)$$

A sketch of the root locus (Fig. 7.43) shows that feedback of altitude by itself does not yield an acceptable design. However, we may also feed back the altitude rate for stabilization. The root locus of the system with h and $\dot{h}$

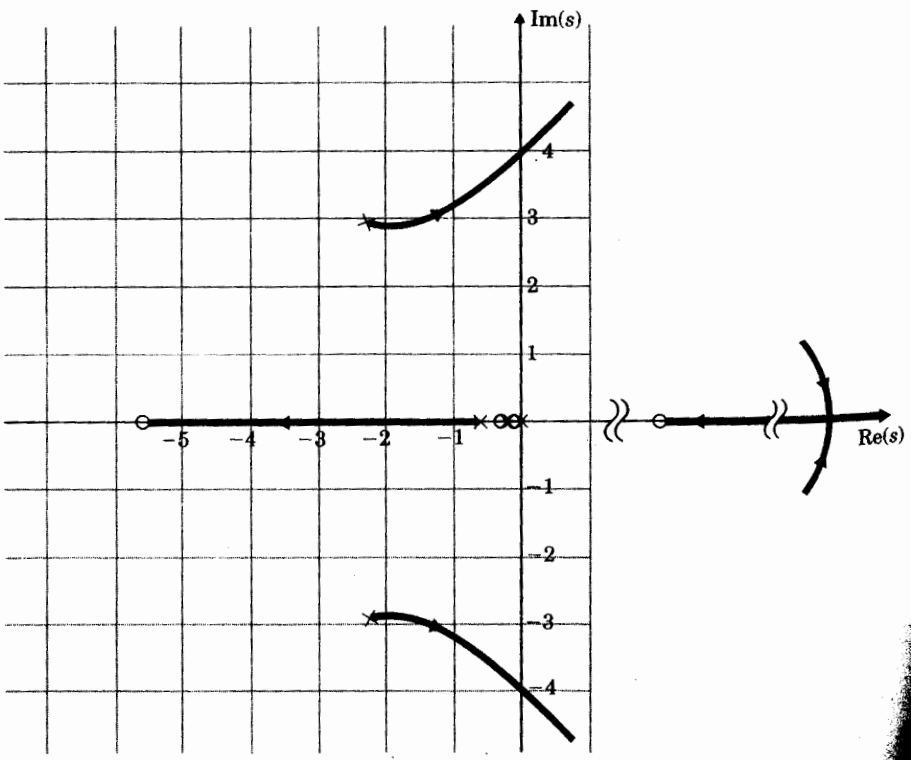

FIGURE 7.44
0° root locus with h and $\dot{h}$ feedback.

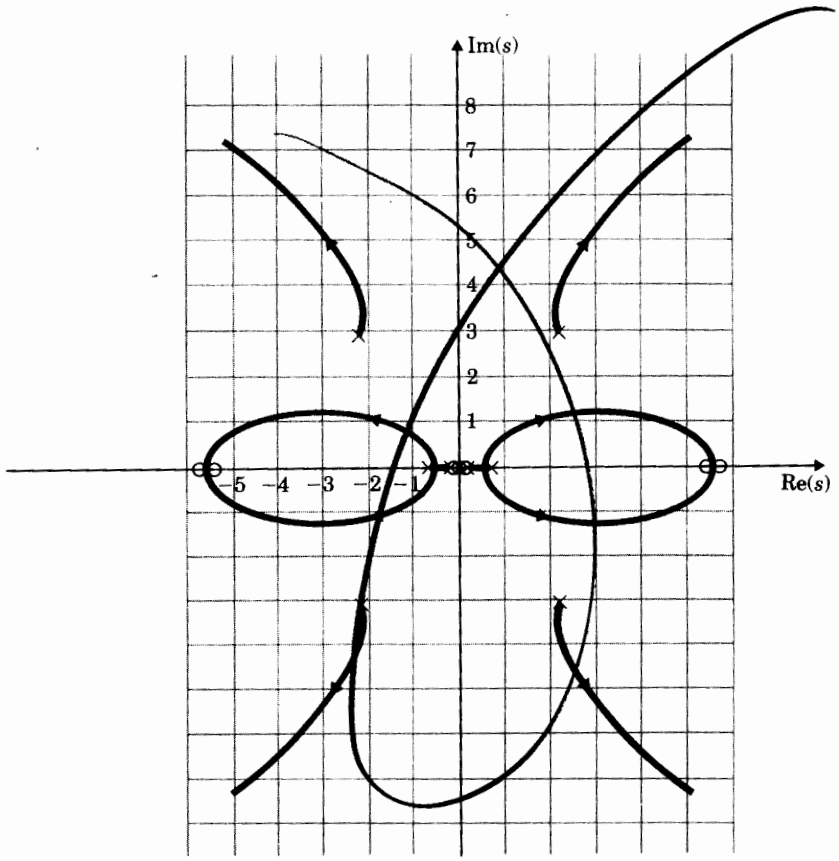

FIGURE 7.45
Symmetric root locus for altitude-hold design.

feedback is shown in Fig. 7.44. The ratio of $\dot{h}$ to h found best after some iteration is 10 : 1; that is,

$$G_e(s) = K_h(s + 0.1).$$

This final design is the result of iterations between the $q, \theta, \dot{h}$, and h feedback gains, obviously a lengthy process. Although this trial design was successful, use of the SRL approach has promise to expedite the process.

STEP 6: *Do an optimal design.* The symmetric root locus of the system is as shown in Fig. 7.45. If we choose the closed loop poles at

$$\alpha_c(s) = (s + 0.0045)(s + 0.145)(s + 0.513)(s + 2.25 \pm j2.98),$$

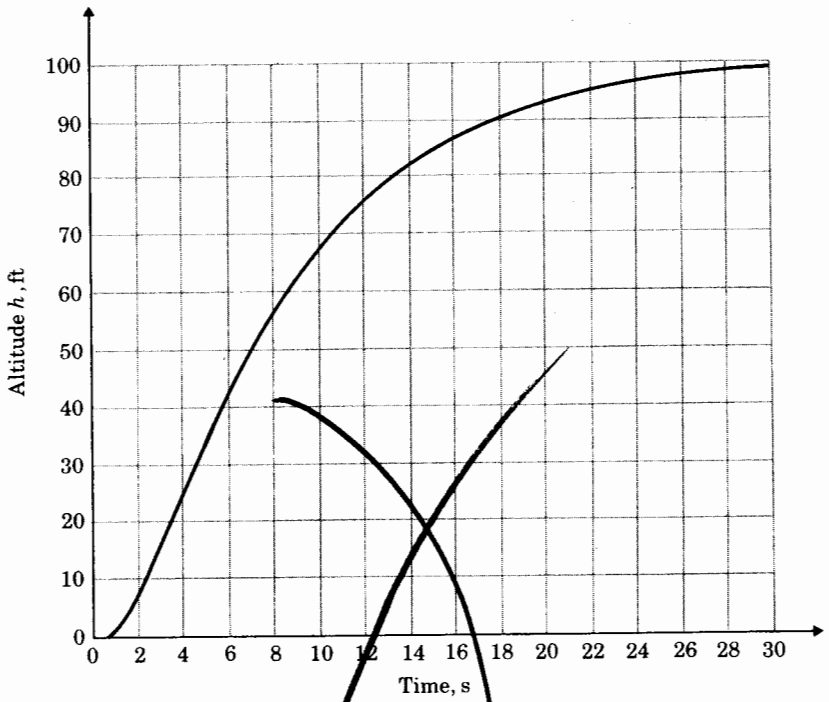

FIGURE 7.46
Step response of altitude-hold autopilot.

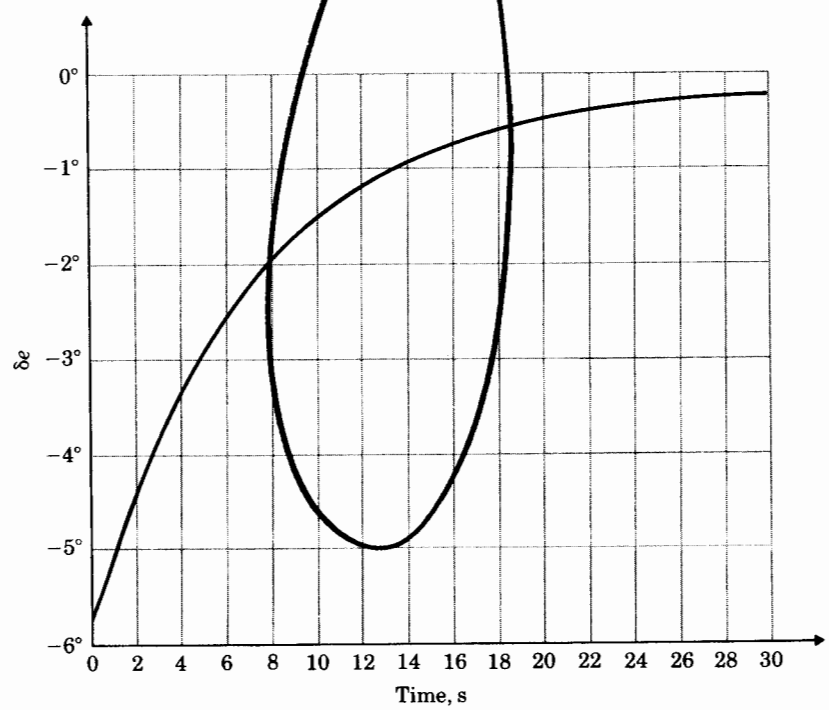

FIGURE 7.47
Control effort for 100-ft step command in altitude.

then the required feedback gain is

$$\mathbf{K} = [-0.0011 \quad 0.0016 \quad -0.0831 \quad -1.6113 \quad -0.001].$$

The step response of the system to a 100-ft step command in h is shown in Fig. 7.46, and the associated control effort is shown in Fig. 7.47.

*7.4 CONTROL OF THE FUEL-AIR RATIO IN AN AUTOMOTIVE ENGINE

Up until the 1980s, most automobile engines had a carburetor to meter the fuel so that the ratio of the gasoline mass flow to air mass flow (F/A) remained in the vicinity of 1 : 15. This device metered the fuel by relying on a pressure drop produced by the air flowing through a venturi. The device has performed adequately for the last 100 years in terms of keeping the engine running satisfactorily, but has historically allowed excursions of up to 20% in the F/A. After the implementation of exhaust-pollution regulations, these F/A excursions were unacceptable. During the 1970s, automobile companies improved the design and manufacturing process of the carburetors so that they became more accurate and delivered an accuracy in the vicinity of 3 to 5%. Through a combination of factors, this improved F/A accuracy helped lower the exhaust pollution to acceptable levels. However, the carburetors were still open-loop devices in that no measurement was made of the F/A that entered the engine for subsequent feedback into the carburetor.

During the 1980s, almost all manufacturers have turned to feedback control systems to provide a much-improved level of F/A accuracy, an action made necessary by the decreasing levels of allowable exhaust pollutants.

As for the other examples, we will discuss each step in the design of this system.

STEP 1: *Understand the process and its performance.* The method chosen to meet the exhaust standards has been to use a catalytic converter that simultaneously oxidizes excess levels of exhaust carbon monoxide (CO) and unburned hydrocarbons (HC) and reduces excess levels of the oxides of nitrogen (NO and NO_2 or NO_x). This device is usually referred to as a "three-way catalyst" because of its effect on all three pollutants. This catalyst is ineffective when the F/A is more than 1% different from the stoichiometric level of 1 : 14.7; therefore, a feedback control system is required to maintain the F/A within $\pm 1\%$ of that desired level. The system is depicted in Fig. 7.48. The dynamic phenomena that affect the relation between the sensed F/A output from the exhaust and the fuel-metering command in the intake manifold are (1) intake fuel and air mixing, (2) cycle delays due to the piston strokes in the engine, and (3) the time required for the exhaust to travel from the engine to the sensor. All these effects are strongly dependent on the speed